Progress In Electromagnetics Research, Vol. 127, 139–154, 2012

ADAPTIVE BEAMFORMING WITH LOW SIDE LOBE LEVEL USING NEURAL NETWORKS TRAINED BY MUTATED BOOLEAN PSO

Z. D. Zaharis*, K. A. Gotsis, and J. N. Sahalos

Radiocommunications Laboratory, Department of Physics, Aristotle University of Thessaloniki, GR-54124 Thessaloniki, Greece

Abstract—A new adaptive beamforming technique based on neural networks (NNs) is proposed. The NN training is accomplished by applying a novel optimization method called Mutated Boolean PSO (MBPSO). In the beginning of the procedure, the MBPSO is repeatedly applied to a set of random cases to estimate the excitation weights of an antenna array that steer the main lobe towards a desired signal, place nulls towards several interference signals and achieve the lowest possible value of side lobe level. The estimated weights are used to train efficiently a NN. Finally, the NN is applied to a new set of random cases and the extracted radiation patterns are compared to respective patterns extracted by the MBPSO and a well-known robust adaptive beamforming technique called Minimum Variance Distortionless Response (MVDR). The aforementioned comparison has been performed considering uniform linear antenna arrays receiving several interference signals and a desired one in the presence of additive Gaussian noise. The comparative results show the advantages of the proposed technique.

1. INTRODUCTION

Smart antenna technology is a very interesting and challenging issue in modern communications [1–3]. One of the major interests concerns the design of antenna arrays that produce radiation patterns dynamically shaped according to certain signal directions that vary with time. In particular, the array must form a main lobe towards a desired incoming signal called signal-of-interest (SOI) and several nulls

Received 28 February 2012, Accepted 6 April 2012, Scheduled 11 April 2012

* Corresponding author: Zaharias D. Zaharis (zaharis@auth.gr).

towards respective undesired or interference incoming signals. Taking into account that the geometry of the array is time-independent, a dynamically shaped pattern is achieved by applying on the array elements appropriate excitation weights that vary with time. These weights are calculated in real time by beamforming techniques [3–17]. Therefore, the beamforming algorithm must be completed as fast as possible.

Our study presents a new adaptive beamforming (ABF) technique suitable for antenna arrays [3–6, 9–17]. The technique is based on neural networks (NNs) [5, 18–26], which use training sets produced by a novel binary variant of Particle Swarm Optimization (PSO) [27–33], called Mutated Boolean PSO (MBPSO) [10]. In the MBPSO, the update of particle velocities and positions is performed using exclusively Boolean expressions, while former binary PSO variants update the particle velocities using real number expressions [34]. Since real number expressions need more CPU time to obtain a result than Boolean expressions, the MBPSO becomes more effective than other binary PSO variants. Moreover, the MBPSO algorithm involves a novel process of adaptive velocity mutation that makes the algorithm more effective than the conventional Boolean PSO [35]. Both the Boolean update mechanism and the adaptive mutation process make the MBPSO a robust algorithm suitable for NN training.

The proposed technique has been applied to uniform linear arrays (ULAs). It starts by selecting a set of random cases where a ULA receives several interference signals and a SOI at respective directions of arrival (DOA) in the presence of additive zero-mean Gaussian noise. The above directions are usually calculated by DOA estimation algorithms [1, 19, 22, 24, 36–40]. The DOA of the SOI and the interference signals represent the input parameters for each case. The MBPSO is applied to each case in order to extract the array excitation weights that steer the main lobe towards the SOI, place nulls towards the interference signals and achieve the lowest possible side lobe level (SLL). These weights are used to train a NN. The NN derived from the training procedure is the actual beamformer. In order to test its effectiveness, a new set of random cases is selected. Then, for every case, the NN is applied to extract the excitation weights and the produced radiation pattern is compared to corresponding patterns extracted by the MBPSO and a well-known robust adaptive beamforming technique called Minimum Variance Distortionless Response (MVDR) [1]. The above comparison shows the advantages of the proposed technique.

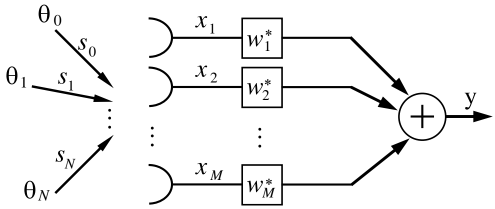

Figure 1. Beamformer block diagram.

2. FORMULATION

The condition described by the beamforming theory [1] is a ULA which is composed of M isotropic sources and receives several monochromatic signals $s_n(k)$ $(n = 0, 1, \ldots, N)$ from respective angles of arrival θ_n $(n = 0, 1, \ldots, N)$. An angle of arrival (AOA) is defined here as the angle between the DOA of a signal and the reference direction which is normal to the ULA axis. The variable k indicates the kth time sample. The signal $s_0(k)$ is the SOI, while $s_n(k)$ $(n = 1, \ldots, N)$ are N interference signals (see Figure 1). The SOI is considered as reference signal in terms of power and thus its mean power is given by:

$$P_s = E\left\{|s_0(k)|^2\right\} = 1 \tag{1}$$

where $E\{\cdot\}$ denotes the mean value. Besides, each mth array element receives an additive zero mean Gaussian noise signal $n_m(k)$ $(m = 1, \ldots, M)$ with variance σ_n^2 calculated from the signal-to-noise ratio SNR in dB as follows:

$$\sigma_n^2 = 10^{-SNR/10} \tag{2}$$

The signal $x_m(k)$ at the input of the mth element can be calculated by the following expression:

$$\bar{x}(k) = \bar{a}_0 s_0(k) + [\bar{a}_1 \quad \bar{a}_2 \quad \ldots \quad \bar{a}_N]\, \bar{s}(k) + \bar{n}(k) \tag{3}$$

where

$$\bar{x}(k) = [x_1(k) \quad x_2(k) \quad \ldots \quad x_M(k)]^T \tag{4}$$

$$\bar{s}(k) = [s_1(k) \quad s_2(k) \quad \ldots \quad s_N(k)]^T \tag{5}$$

$$\bar{n}(k) = [n_1(k) \quad n_2(k) \quad \ldots \quad n_M(k)]^T \tag{6}$$

are, respectively, the input vector, the interference vector and the noise vector, while

$$\bar{a}_n = \left[1 \quad e^{j\frac{2\pi}{\lambda}q\sin\theta_n} \quad \ldots \quad e^{j(M-1)\frac{2\pi}{\lambda}q\sin\theta_n}\right]^T, \quad n = 0, 1, \ldots, N \tag{7}$$

is the array steering vector at AOA θ_n. Also, the superscript T indicates the transpose operation. In (7), q is the distance between adjacent elements of the ULA and λ is the wavelength. Equation (3) can be written in the following form:

$$\bar{x}(k) = \bar{a}_0 s_0(k) + \bar{A}\bar{s}(k) + \bar{n}(k) = \bar{x}_d(k) + \bar{x}_u(k) \tag{8}$$

where $\bar{A} = [\bar{a}_1 \ \bar{a}_2 \ \ldots \ \bar{a}_N]$ is an $M \times N$ matrix called array steering matrix. The vectors

$$\bar{x}_d(k) = \bar{a}_0 s_0(k) \tag{9}$$

$$\bar{x}_u(k) = \bar{A}\bar{s}(k) + \bar{n}(k) \tag{10}$$

are respectively the vector of the desired input signals and the vector of the undesired (interference plus noise) input signals. According to Figure 1, the array output is calculated as follows:

$$y(k) = \bar{w}^H \bar{x}(k) = \bar{w}^H \bar{x}_d(k) + \bar{w}^H \bar{x}_u(k) \tag{11}$$

where $\bar{w} = [w_1 \ w_2 \ \ldots \ w_M]^T$ is the excitation weight vector and the superscript H indicates the Hermitian transpose operation. Equation (11) can be written in the following form:

$$y(k) = y_d(k) + y_u(k) \tag{12}$$

where

$$y_d(k) = \bar{w}^H \bar{x}_d(k) \tag{13}$$

$$y_u(k) = \bar{w}^H \bar{x}_u(k) \tag{14}$$

are, respectively, the desired and the undesired component of the array output. The mean power of $y_d(k)$ is expressed as:

$$\sigma_d^2 = E\left\{\left|\bar{w}^H \bar{x}_d(k)\right|^2\right\} = E\left\{\left|\bar{w}^H \bar{a}_0 s_0(k)\right|^2\right\} = \bar{w}^H \bar{a}_0 \bar{a}_0^H \bar{w} \tag{15}$$

Also, the mean power of $y_u(k)$ is expressed as:

$$\begin{aligned}\sigma_u^2 &= E\left\{\left|\bar{w}^H \bar{x}_u(k)\right|^2\right\} = E\left\{\left|\bar{w}^H \left[\bar{A}\bar{s}(k) + \bar{n}(k)\right]\right|^2\right\} \\ &= \bar{w}^H \bar{A}\bar{R}_i \bar{A}^H \bar{w} + \bar{w}^H \bar{R}_n \bar{w}\end{aligned} \tag{16}$$

where $\bar{R}_i = E\{\bar{s}(k)\,\bar{s}^H(k)\}$ and $\bar{R}_n = E\{\bar{n}(k)\,\bar{n}^H(k)\}$ are respectively the interference correlation matrix and the noise correlation matrix. Given that $\bar{n}(k)$ consists of uncorrelated zero-mean noise signals, it results $\bar{R}_n = \sigma_n^2 I$. Thus, (16) can be written in the following form:

$$\sigma_u^2 = \bar{w}^H \bar{A}\bar{R}_i \bar{A}^H \bar{w} + \sigma_n^2 \bar{w}^H \bar{w} \tag{17}$$

One of the parameters used to measure the effectiveness of a beamformer is the signal-to-interference-plus-noise ratio (*SINR*). Due to (15) and (17), *SINR* can be calculated by:

$$SINR = \frac{\sigma_d^2}{\sigma_u^2} = \frac{\bar{w}^H \bar{a}_0 \bar{a}_0^H \bar{w}}{\bar{w}^H \bar{A}\bar{R}_i \bar{A}^H \bar{w} + \sigma_n^2 \bar{w}^H \bar{w}} \tag{18}$$

The basic process performed by the MBPSO is the minimization of a fitness function F. The inverse of $SINR$ could be used as an expression of F. As F is minimized, $SINR$ is maximized, meaning that the main lobe is steered towards the SOI and nulls are formed towards the interference signals. Our technique becomes more challenging by setting an additional requirement which is the minimization of the SLL. Taking into account the above considerations, F can be described by the following expression:

$$F = \gamma_1 \frac{\bar{w}^H \bar{A} \bar{R}_i \bar{A}^H \bar{w} + \sigma_n^2 \bar{w}^H \bar{w}}{\bar{w}^H \bar{a}_0 \bar{a}_0^H \bar{w}} + \gamma_2 SLL \tag{19}$$

where coefficients γ_1 and γ_2 are used to balance the minimization of the two terms given in (19).

3. MUTATED BOOLEAN PSO

The Boolean PSO (BPSO) is a binary PSO variant described in [35]. The MBPSO is a novel version of BPSO proposed by the authors [10].

In the BPSO and MBPSO, the position X_s and the velocity V_s ($s = 1, \ldots, S$) of every particle of the swarm are represented by J-bit strings. The search space is defined by an upper and a lower boundary. A large fitness value is assigned as a penalty to particles being outside the search space. Provided that the optimization process minimizes the fitness function, these particles are gradually moved inside the search space.

An important novelty found only in the BPSO and MBPSO is the exclusively Boolean update of X_s and V_s given below:

$$v_{js} = r_1 \cdot v_{js} + r_2 \cdot (p_{js} \oplus x_{js}) + r_3 \cdot (g_j \oplus x_{js}) \tag{20}$$

$$x_{js} = x_{js} \oplus v_{js} \tag{21}$$

where $\cdot$, $+$ and $\oplus$ are respectively the "*and*", "*or*" and "*xor*" operators, x_{js} and v_{js} are respectively the jth bit of X_s and V_s, p_{js} is the jth bit of the best position P_s found so far by the sth particle and g_j is the jth bit of the best position G found so far by the swarm. Moreover, r_1, r_2, and r_3 are random bits and their probabilities of being '1' are respectively defined by the parameters R_1, R_2, and R_3. The exclusively Boolean update makes both the BPSO and MBPSO more effective than a well-known binary PSO (binPSO) variant that uses real number update expressions as described in [34].

Both the BPSO and MBPSO control the convergence speed of the process by controlling the *velocity length* l_s which is the number of '1's in V_s and is not permitted to exceed an upper limit $l_{\max}$. Therefore, if $l_s > l_{\max}$ then randomly chosen '1's in V_s change into '0's until $l_s = l_{\max}$.

To increase the exploration ability of the swarm, an adaptive mutation process applied to particle velocities has been involved in the MBPSO. This novelty makes the MBPSO more effective than the typical BPSO. According to this process, every '0' in V_s may change to '1' with *mutation probability* m_p, which linearly decreases as follows:

$$m_p(i) = m_{p0} \frac{i_{\text{tot}} - i}{i_{\text{tot}} - 1}, \quad i = 1, \ldots, i_{\text{tot}} \tag{22}$$

where i is the current iteration number, i_{tot} is the total number of iterations and m_{p0} is the initial value of m_p. Usually, m_{p0} has relatively small values to avoid pure random search. Comparative convergence graphs presented below in section 6 exhibit the superiority of the MBPSO in comparison to the typical BPSO and the binPSO proposed in [34].

The MBPSO is an iterative technique and like every evolutionary technique is time-consuming. Nevertheless, this problem is not crucial because the MBPSO is used here only for NN training which is not a real time procedure. The real time procedure is performed by the trained NN which responds very fast.

4. MINIMUM VARIANCE DISTORTIONLESS RESPONSE

The Minimum Variance Distortionless Response (MVDR) is a robust adaptive beamforming method that aims at minimizing the mean power of $y_u(k)$, while $y_d(k)$ is preserved [1]. Thus, the optimum excitation weight vector is derived by minimizing the quantity $\bar{w}^H \bar{R}_u \bar{w}$, while $\bar{w}^H \bar{a}_0 = 1$, and is given by:

$$\bar{w}_{mvdr} = \frac{\bar{R}_u^{-1} \bar{a}_0}{\bar{a}_0^H \bar{R}_u^{-1} \bar{a}_0} \tag{23}$$

where

$$\bar{R}_u = E\left\{\bar{x}_u(k)\, \bar{x}_u^H(k)\right\} = \bar{A}\bar{R}_i\bar{A}^H + \sigma_n^2 I \tag{24}$$

is the correlation matrix of $y_u(k)$.

5. NN-MBPSO BASED ADAPTIVE BEAMFORMING

A NN is a structure of interconnected information processing units, called neurons, organized in layers [18]. During the training of a NN, the weight connections of its neurons properly change in order to model

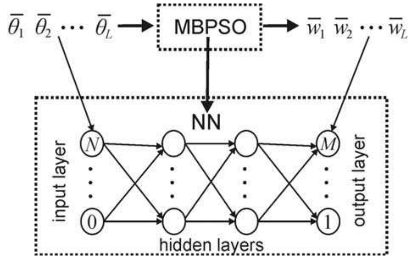

Figure 2. Block diagram illustrating the NN structure and the NN-MBPSO based adaptive beamforming methodology.

the mapping between certain inputs and their respective outputs. NNs have been broadly applied in various problems of electromagnetics and mobile communications [5, 18–26]. Due to their fast response and easy implementation, NNs constitute an attractive solution for real time applications, such as beamforming and DOA estimation [5, 19, 22, 24].

In the proposed ABF technique, the NNs are trained by L randomly generated angle vectors $\bar{\theta}_l = [\theta_{0l}\ \theta_{1l}\ \ldots\ \theta_{Nl}]^T$ paired with the respective optimal excitations weight vectors $\bar{w}_l = [w_{1l}\ w_{2l}\ \ldots\ w_{Ml}]^T$. The first element of the lth angle vector, θ_{0l}, is the AOA of the SOI, while the other elements, θ_{nl} ($n = 1, \ldots, N$), are the AOA of the interference signals. The weight vectors are optimized by applying the MBPSO on the fitness function given in (19).

The L randomly created pairs ($\bar{\theta}_l$, $\bar{w}_l$) constitute a set employed for the supervised training of a feedforward Multilayer Perceptron (MLP) NN [18]. The training takes place in MATLAB® R2010a environment, using a very efficient implementation of the fast and effective Levenberg-Marquardt backpropagation algorithm [41]. Figure 2 illustrates the proposed ABF method, giving also the NN structure. The NN is composed by (a) an input layer of $N + 1$ nodes fed by the angle vectors, (b) two hidden layers and (c) an output layer of M nodes that gives the corresponding weight vectors. The number of nodes for each hidden layer depends on the number of training pairs and the dimension of the angle vector. The criterion of their choice is the better NN training performance and the accuracy of the results. More details about NN training using the Levenberg-Marquardt backpropagation algorithm in MATLAB can be found in [19].

The introduced NN-MBPSO based adaptive beamforming methodology is summarized in the following steps:

1. Random generation of L angle vectors $\bar{\theta}_l$ denoting the AOA of the SOI and the interference signals.
2. Production of the optimal $\bar{w}_l$ that correspond to $\bar{\theta}_l$ using the

MBPSO algorithm.

3. Creation of a MLP NN and back propagation training using the collection of the randomly created pairs $(\bar{\theta}_l, \bar{w}_l)$, $l = 1, 2, \ldots, L$.
4. The trained NN instantly responds to any input angle vector, giving as output the excitation weight vector that makes the antenna array produce a radiation pattern with the desired characteristics concerning the main lobe, the nulls and the SLL.

6. NUMERICAL RESULTS

Three different scenarios are considered to test the performance of the proposed technique. The first two scenarios concern a 9-element ULA ($M = 9$) with $q = 0.5\lambda$ and $SNR = 10\,\text{dB}$ receiving respectively three ($N = 3$) and five ($N = 5$) interference signals, while the third scenario concerns a 7-element ULA ($M = 7$) with $q = 0.5\lambda$ and $SNR = 10\,\text{dB}$ receiving three ($N = 3$) interference signals. The parameters used by the MBPSO in all the scenarios were: $S = 20$, $R_1 = 0.1$, $R_2 = 0.5$, $R_3 = 0.5$, $l_{\max} = 4$, $m_{p0} = 0.10$, and $i_{\text{tot}} = 500$. A set of 5000 random cases ($L = 5000$) is selected for each scenario. Each case is a group of $N + 1$ values randomly selected from a uniform angle distribution and given respectively to θ_n ($n = 0, 1, \ldots, N$).

Initially, a comparison in terms of convergence among the MBPSO, the conventional BPSO and the binary PSO (binPSO) proposed in [34] is made. Thus, the three methods are applied to each one of the 5000 cases of the first scenario to extract the corresponding $\bar{w}$. The convergence graphs of the three methods are recorded for each case. In this way, comparative graphs showing the average convergence are constructed (see Figure 3). It is obvious that the MBPSO converges a little slower than the BPSO, but it finally achieves better fitness

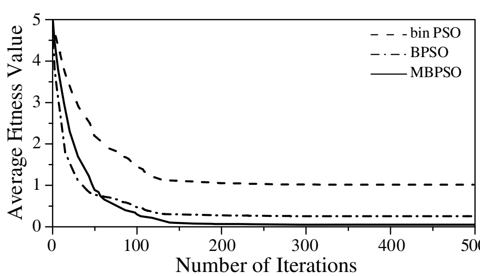

Figure 3. Comparative graphs showing the average convergence of the MBPSO, the conventional BPSO and the binary PSO (binPSO) proposed in [34].

values. Moreover, the MBPSO converges faster and achieves better fitness values than the binPSO. The above comparison justifies the use of MBPSO-based data to train a NN.

The excitation weight vectors extracted by the MBPSO for the 5000 random cases of each scenario are used to train a NN. The trained NN is compared to the MBPSO and MVDR in terms of performance by selecting a new set of 1000 random cases. Then, the three algorithms are applied to each case to extract the excitation weight vectors, respectively $\bar{w}_{NN}$, $\bar{w}_{MBPSO}$ and $\bar{w}_{MVDR}$, as well as the corresponding radiation patterns produced by these vectors. The weights of each vector are normalized with reference to the weight of the middle element of the array. The amplitudes of all the weights found by the above procedure range from 0.05 to 2.

The 1000 patterns derived by the NN are statistically analyzed for each scenario regarding the absolute divergence $\Delta\theta_{\text{main}}$ of the main lobe direction from its desired value θ_0 as well as the absolute divergence $\Delta\theta_{\text{null}}$ of the null directions from their respective desired values θ_n $(n = 1, \ldots, N)$. The statistical results are illustrated in Figures 4, 5

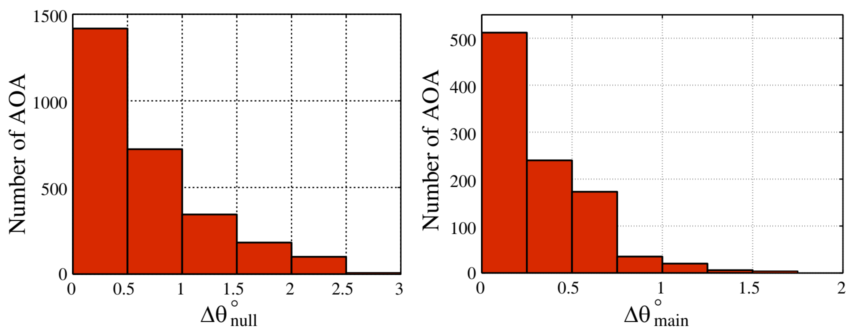

Figure 4. Statistical distributions of the main lobe and null angular divergences derived from the NN for the 1st scenario ($M = 9$, $N = 3$).

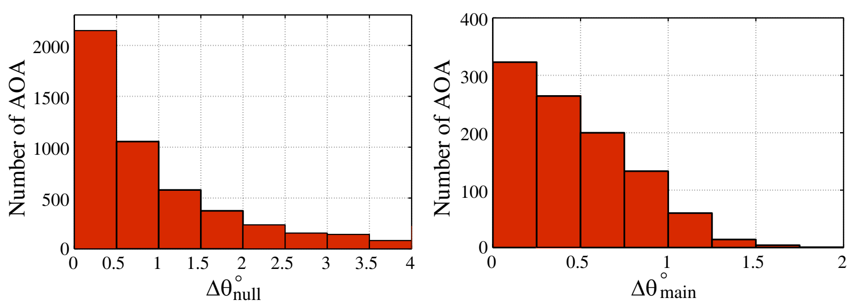

Figure 5. Statistical distributions of the main lobe and null angular divergences derived from the NN for the 2nd scenario ($M = 9$, $N = 5$).

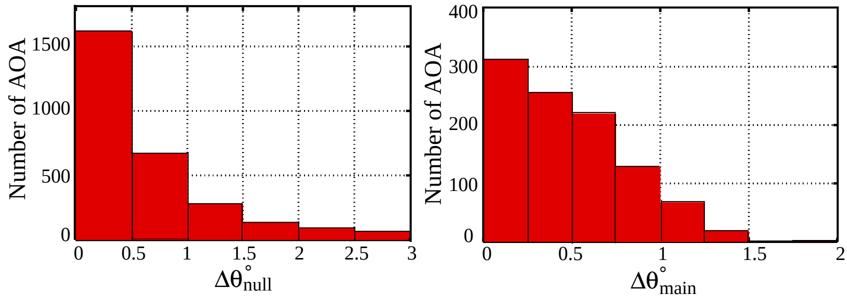

Figure 6. Statistical distributions of the main lobe and null angular divergences derived from the NN for the 3rd scenario ($M = 7$, $N = 3$).

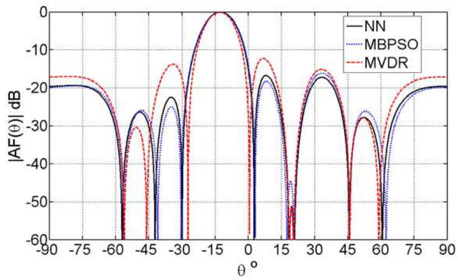

Figure 7. Optimal patterns for $SNR = 10\,\text{dB}$, $M = 9$, a SOI arriving from $\theta_0 = -13°$, and three interference signals arriving from AOA $-56°$, $20°$ and $46°$ ($SINR_{NN} = 19.16\,\text{dB}$, $SINR_{MBPSO} = 19.14\,\text{dB}$, $SINR_{MVDR} = 19.35\,\text{dB}$, $SLL_{NN} = -16.73\text{dB}$, $SLL_{MBPSO} = -16.15\,\text{dB}$, $SLL_{MVDR} = -12.23\,\text{dB}$, $D_{NN} = 9.35\,\text{dB}$, $D_{MBPSO} = 9.35\,\text{dB}$, $D_{MVDR} = 9.32\,\text{dB}$).

Table 1. Average angular divergence and average SLL values.

Scenario	1st	2nd	3rd
M	9	9	7
N	3	5	3
$\overline{\Delta\theta}_{\text{main}}$	0.33°	0.46°	0.47°
$\overline{\Delta\theta}_{\text{null}}$	0.75°	0.95°	0.73°
$\overline{SLL}_{NN}$	-13.61 dB	-13.28 dB	-12.57 dB
$\overline{SLL}_{MBPSO}$	-13.44 dB	-13.18 dB	-12.55 dB
$\overline{SLL}_{MVDR}$	-12.26 dB	-11.74 dB	-11.25 dB

and 6. Considering a confidence level of 5% for all the scenarios, the main lobe divergence is less than 1° and the null divergence is less than 2°. The above analysis as well as the average absolute divergence values $\overline{\Delta\theta}_{\text{main}}$ and $\overline{\Delta\theta}_{\text{null}}$ given in Table 1 show that the NN has a high percentage of success in steering both the main lobe and the nulls.

In addition, the above set of 1000 patterns derived by the trained NN is used to calculate the average SLL value denoted as $\overline{SLL_{NN}}$. Respective values, $\overline{SLL_{MBPSO}}$ and $\overline{SLL_{MVDR}}$, are calculated from two similar sets of 1000 patterns derived by the MBPSO and the MVDR.

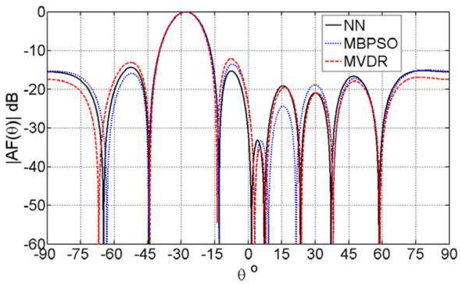

Figure 8. Optimal patterns for $SNR = 10\,\text{dB}$, $M = 9$, a SOI arriving from $\theta_0 = -28°$, and five interference signals arriving from AOA $-44°$, $-13°$, $3°$, $38°$ and $59°$ ($SINR_{NN} = 18.91\,\text{dB}$, $SINR_{MBPSO} = 18.93\,\text{dB}$, $SINR_{MVDR} = 18.76\,\text{dB}$, $SLL_{NN} = -14.34\,\text{dB}$, $SLL_{MBPSO} = -13.48\,\text{dB}$, $SLL_{MVDR} = -12.11\,\text{dB}$, $D_{NN} = 9.45\,\text{dB}$, $D_{MBPSO} = 9.45\,\text{dB}$, $D_{MVDR} = 9.43\,\text{dB}$).

Table 2. Normalized optimal weight values for $SNR = 10\,\text{dB}$, $M = 9$, a SOI arriving from $\theta_0 = -13°$, and three interference signals arriving from AOA $-56°$, $20°$ and $46°$.

m	w_{NN}	w_{MBPSO}	w_{MVDR}
1	$-0.553 + j0.277$	$-0.525 + j0.285$	$-1.179 + j0.479$
2	$-0.332 + j0.657$	$-0.302 + j0.585$	$-0.735 + j1.254$
3	$0.205 + j1.059$	$0.223 + j1.000$	$0.344 + j1.837$
4	$0.930 + j0.903$	$0.917 + j0.887$	$1.378 + j1.325$
5	$1.000 + j0$	$1.000 + j0$	$1.000 + j0$
6	$0.930 - j0.903$	$0.917 - j0.887$	$1.378 - j1.325$
7	$0.205 - j1.059$	$0.223 - j1.000$	$0.344 - j1.837$
8	$-0.332 - j0.657$	$-0.302 - j0.585$	$-0.735 - j1.254$
9	$-0.553 - j0.277$	$-0.525 - j0.285$	$-1.179 - j0.479$

Table 3. Normalized optimal weight values for $SNR = 10\,\text{dB}$, $M = 9$, a SOI arriving from $\theta_0 = -28°$, and five interference signals arriving from AOA $-44°$, $-13°$, $3°$, $38°$ and $59°$.

m	w_{NN}	w_{MBPSO}	w_{MVDR}
1	$0.841 - j0.229$	$0.733 - j0.264$	$0.974 - j0.328$
2	$-0.447 - j0.824$	$-0.469 - j0.759$	$-0.495 - j1.071$
3	$-1.023 + j0.239$	$-1.000 + j0.153$	$-1.294 + j0.256$
4	$0.009 + j1.137$	$-0.019 + j1.000$	$-0.026 + j1.231$
5	$1.000 + j0$	$1.000 + j0$	$1.000 + j0$
6	$0.009 - j1.137$	$-0.019 - j1.000$	$-0.026 - j1.231$
7	$-1.023 - j0.239$	$-1.000 - j0.153$	$-1.294 - j0.256$
8	$-0.447 + j0.824$	$-0.469 + j0.759$	$-0.495 + j1.071$
9	$0.841 + j0.229$	$0.733 + j0.264$	$0.974 + j0.328$

These values are given in Table 1. It seems that $\overline{SLL}_{NN}$ approaches $\overline{SLL}_{MBPSO}$ but it is better than $\overline{SLL}_{MVDR}$. Both facts are predictable because the NN is trained by the MBPSO, which takes into account the *SLL* minimization as shown in (19), while the MVDR does not. Thus, in many cases the NN produces notably better *SLL* values than the MVDR. Such cases are shown in Figures 7 and 8. The values of *SINR*, *SLL* and directivity D, derived from each case, are given in the legend of the respective figure. Also, the normalized optimal weight values are given respectively in Tables 2 and 3.

7. CONCLUSION

A new robust ABF method, that combines the optimization capabilities of the MBPSO with the speed and efficiency of NNs, has been developed. NNs have been trained by optimal training sets derived by the MBPSO, in order to learn to produce the proper excitation weight vectors that make the array steer the main lobe towards the SOI and form nulls towards the interference signals. Emphasis has been given to the production of radiation patterns with lower *SLL* compared to the MVDR, which is a popular ABF technique. Extensive simulation results prove the generalization capabilities of the properly trained NNs and show that the proposed NN-MBPSO based adaptive beamforming methodology succeeds the above mentioned goals.

The cases studied here show that the MBPSO converges a little slower than the BPSO and faster than the binPSO, and also achieves better fitness values than both the BPSO and binPSO. The CPU time required by the MBPSO to converge and the NN training is not an issue, since neither the MBPSO nor the training is involved in the real time procedure of the actual beamformer. After its training the NN responds instantly. Therefore, the proposed beamformer seems to be quite promising in the smart antenna technology.

REFERENCES

1. Gross, F. B., *Smart Antennas for Wireless Communications with Matlab*, McGraw-Hill, New York, 2005.
2. Viani, F., L. Lizzi, M. Donelli, D. Pregnolato, G. Oliveri, and A. Massa, "Exploitation of parasitic smart antennas in wireless sensor networks," *Journal of Electromagnetic Waves and Applications*, Vol. 24, No. 7, 993–1003, 2010.
3. Jabbar, A. N., "A novel ultra-fast ultra-simple adaptive blind beamforming algorithm for smart antenna arrays," *Progress In Electromagnetics Research B*, Vol. 35, 329–348, 2011.
4. Li, J. and P. Stoica, *Robust Adaptive Beamforming*, John Wiley & Sons, Inc., Hoboken, New Jersey, 2006.
5. Castaldi, G., V. Galdi, and G. Gerini, "Evaluation of a neural-network-based adaptive beamforming scheme with magnitude-only constraints," *Progress In Electromagnetics Research B*, Vol. 11, 1–14, 2009.
6. Umrani, A. W., Y. Guan, and F. A. Umrani, "Effect of steering error vector and angular power distributions on beamforming and transmit diversity systems in correlated fading channel," *Progress In Electromagnetics Research*, Vol. 105, 383–402, 2010.
7. Byrne, D., M. O'Halloran, M. Glavin, and E. Jones, "Data independent radar beamforming algorithms for breast cancer detection," *Progress In Electromagnetics Research*, Vol. 107, 331–348, 2010.
8. Byrne, D., M. O'Halloran, E. Jones, and M. Glavin, "Transmitter-grouping robust capon beamforming for breast cancer detection," *Progress In Electromagnetics Research*, Vol. 108, 401–416, 2010.
9. Lee, J.-H., Y.-S. Jeong, S.-W. Cho, W.-Y. Yeo, and K. S. J. Pister, "Application of the newton method to improve the accuracy of TOA estimation with the beamforming algorithm and the music algorithm," *Progress In Electromagnetics Research*, Vol. 116, 475–515, 2011.

10. Zaharis, Z. D. and T. V. Yioultsis, "A novel adaptive beamforming technique applied on linear antenna arrays using adaptive mutated boolean PSO," *Progress In Electromagnetics Research*, Vol. 117, 165–179, 2011.
11. Mallipeddi, R., J. P. Lie, P. N. Suganthan, S. G. Razul, and C. M. S. See, "A differential evolution approach for robust adaptive beamforming based on joint estimation of look direction and array geometry," *Progress In Electromagnetics Research*, Vol. 119, 381–394, 2011.
12. Mallipeddi, R., J. P. Lie, P. N. Suganthan, S. G. Razul, and C. M. S. See, "Near optimal robust adaptive beamforming approach based on evolutionary algorithm," *Progress In Electromagnetics Research B*, Vol. 29, 157–174, 2011.
13. Lee, J.-H., G.-W. Jung, and W.-C. Tsai, "Antenna array beamforming in the presence of spatial information uncertainties," *Progress In Electromagnetics Research B*, Vol. 31, 139–156, 2011.
14. Lee, J.-H., "Robust antenna array beamforming under cycle frequency mismatch," *Progress In Electromagnetics Research B*, Vol. 35, 307–328, 2011.
15. Liu, Y., Q. Wan, and X. Chu, "A robust beamformer based on weighted sparse constraint," *Progress In Electromagnetics Research Letters*, Vol. 16, 53–60, 2010.
16. Liu, Y. and Q. Wan, "Total difference based partial sparse LCMV beamformer," *Progress In Electromagnetics Research Letters*, Vol. 18, 97–103, 2010.
17. Mallipeddi, R., J. P. Lie, S. G. Razul, P. N. Suganthan, and C. M. S. See, "Robust adaptive beamforming based on covariance matrix reconstruction for look direction mismatch," *Progress In Electromagnetics Research Letters*, Vol. 25, 37–46, 2011.
18. Christodoulou, C. and M. Georgiopoulos, *Applications of Neural Networks in Electromagnetics*, Artech House, Boston-London, 2001.
19. Gotsis, K. A., K. Siakavara, and J. N. Sahalos, "On the direction of arrival (DoA) estimation for a switched-beam antenna system using neural networks," *IEEE Transactions on Antennas and Propagation*, Vol. 57, No. 5, 1399–1411, May 2009.
20. Bregains, J. C., J. Dorado, M. Gestal, J. A. Rodriguez, F. Ares, and A. Pazos, "Avoiding interference in planar arrays through the use of artificial neural networks," *IEEE Antennas and Propagation Magazine*, Vol. 44, No. 4, 61–65, August 2002.

21. Luo, M. and K.-M. Huang, "Prediction of the electromagnetic field in metallic enclosures using artificial neural networks," *Progress In Electromagnetics Research*, Vol. 116, 171–184, 2011.
22. Kim, Y. and H. Ling, "Direction of arrival estimation of humans with a small sensor array using an artificial neural network," *Progress In Electromagnetics Research B*, Vol. 27, 127–149, 2011.
23. Vakula, D. and N. V. S. N. Sarma, "Using neural networks for fault detection in planar antenna arrays," *Progress In Electromagnetics Research Letters*, Vol. 14, 21–30, 2010.
24. Peng, H., Z. Yang, and T. Yang, "Calibration of a six-port receiver for direction finding using the artificial neural network technique," *Progress In Electromagnetics Research Letters*, Vol. 27, 17–24, 2011.
25. Sacha, G. M., F. B. Rodríguez, E. Serrano, and P. Varona, "Generalized image charge method to calculate electrostatic magnitudes at the nanoscale powered by artificial neural networks," *Journal of Electromagnetic Waves and Applications*, Vol. 24, Nos. 8–9, 1145–1155, 2010.
26. Guo, L. and L. Parsa, "Geometry optimization of IPM machines using orthogonal experimental design method and artificial neural network," *Journal of Electromagnetic Waves and Applications*, Vol. 25, No. 7, 901–912, 2011.
27. Carro Ceballos, P. L., J. De Mingo Sanz, and P. G. Dúcar, "Radiation pattern synthesis for maximum mean effective gain with spherical wave expansions and particle swarm techniques," *Progress In Electromagnetics Research*, Vol. 103, 355–370, 2010.
28. Zhang, Y., S. Wang, and L. Wu, "A novel method for magnetic resonance brain image classification based on adaptive chaotic PSO," *Progress In Electromagnetics Research*, Vol. 109, 325–343, 2010.
29. Wang, W.-B., Q. Feng, and D. Liu, "Application of chaotic particle swarm optimization algorithm to pattern synthesis of antenna arrays," *Progress In Electromagnetics Research*, Vol. 115, 173–189, 2011.
30. Li, W.-T., Y.-Q. Hei, and X.-W. Shi, "Pattern synthesis of conformal arrays by a modified particle swarm optimization," *Progress In Electromagnetics Research*, Vol. 117, 237–252, 2011.
31. Liu, D., Q. Feng, W.-B. Wang, and X. Yu, "Synthesis of unequally spaced antenna arrays by using inheritance learning particle swarm optimization," *Progress In Electromagnetics Research*, Vol. 118, 205–221, 2011.

32. Wang, D., H. Zhang, T. Xu, H. Wang, and G. Zhang, "Design and optimization of equal split broadband microstrip Wilkinson power divider using enhanced particle swarm optimization algorithm," *Progress In Electromagnetics Research*, Vol. 118, 321–334, 2011.
33. Lin, D.-B., F.-N. Wu, W. S. Liu, C. K. Wang, and H.-Y. Shih, "Crosstalk and discontinuities reduction on multi-module memory bus by particle swarm optimization," *Progress In Electromagnetics Research*, Vol. 121, 53–74, 2011.
34. Kennedy, J. and R. C. Eberhart, "A discrete binary version of the particle swarm algorithm," *Proc. World Multiconference on Systemics, Cybernetics and Informatics*, 4104–4109, 1997.
35. Afshinmanesh, F., A. Marandi, and M. Shahabadi, "Design of a single-feed dual-band dual-polarized printed microstrip antenna using a Boolean particle swarm optimization," *IEEE Transactions on Antennas and Propagation*, Vol. 56, No. 7, 1845–1852, July 2008.
36. Yang, P., F. Yang, and Z.-P. Nie, "DOA estimation with sub-array divided technique and interporlated esprit algorithm on a cylindrical conformal array antenna," *Progress In Electromagnetics Research*, Vol. 103, 201–216, 2010.
37. Park, G. M., H. G. Lee, and S. Y. Hong, "Doa resolution enhancement of coherent signals via spatial averaging of virtually expanded arrays," *Journal of Electromagnetic Waves and Applications*, Vol. 24, No. 1, 61–70, 2010.
38. Lui, H. S. and H. T. Hui, "Effective mutual coupling compensation for direction-of-arrival estimations using a new, accurate determination method for the receiving mutual impedance," *Journal of Electromagnetic Waves and Applications*, Vol. 24, Nos. 2–3, 271–281, 2010.
39. Liang, J. and D. Liu, "Two L-shaped array-based 2-D DOAs estimation in the presence of mutual coupling," *Progress In Electromagnetics Research*, Vol. 112, 273–298, 2011.
40. Bencheikh, M. L. and Y. Wang, "Combined esprit-rootmusic for DOA-dod estimation in polarimetric bistatic MIMO radar," *Progress In Electromagnetics Research Letters*, Vol. 22, 109–117, 2011.
41. Neural Network Toolbox™ User's Guide R2010a, MATLAB®, The MathWorks, Inc.